Lab Report 3

Flow Characterization in Urban Development

ASE120K: Low-Speed Aerodynamics Lab

Instructor/Teaching Assistant: Mustafa Musta/John Murray

The University of Texas at Austin

Department of Aerospace Engineering and Engineering Mechanics

Spring 2022

By including my name on the front page of this lab report, I acknowledge that I have read this entire document prior to submission, that I approve of all material contained in this document, and that this is an original and non-plagiarized work of all members of my group.

Group #2: Shreyashee Bhattacharjee, Aubrey Baker, Mark Dunn, Gregory Walters

EIDs: sb57454, alb6443, mad5629, gww532

Due Friday, 06 May 2022

Contents

1 Abstract

The focus of this experimental study was to explore the flow behavior in a city to better understand its impact on pedestrians as well as low-flying aircraft, such as drones. In order to do this, a city model was constructed out of four model buildings of 100.22:1 scale placed in a 2x2 grid formation. The model was placed in a wind tunnel and observed at a Reynolds number of 95625 $\pm$ 375. To interpret and characterize the flow, a smoke wand was used to visualize the flow at different altitudes. The observations from this experiment remain consistent with literature; venturi and upwash effects, among others, can be seen to be characterizing the behavior of the flow. In order to develop an idea of what the velocities look like in a city, a pitot rake was used to create a wake velocity profile of the flow downstream of the building formation. The funnel effect is demonstrated in the wake velocity profile by the higher flow velocity in the "corridor region" between buildings. The velocity profile also demonstrates oscillatory behavior that goes beyond the scope of this experimental analysis.

2 Introduction

For every 1% growth in the global economy, there is a 1% growth in skyscrapers as well [2]. Since tall structures can cause drastic changes in local wind patterns, these skyscrapers can have a negative impact on pedestrian comfort. Pedestrian level wind [3] can impact local businesses and services, as well as pedestrian comfort and safety. Notable buildings and cities that have been known to experience hazardous wind environments at the pedestrian level include the 20 Fenchurch Street skyscraper in London, New York City, and Toronto [9].

Pedestrian wind comfort is a subset of wind engineering that studies the impact of wind on pedestrian-level comfort and safety at a height of 1.5 meters above ground. More specifically, wind engineers study wind flow characteristics and their interaction with civil development. Acceptable limits of pedestrian-level wind have been identified as follows: standing 3.8 m/s and cycling 5.5 m/s [3].

Dense urban areas with skyscrapers make pedestrians susceptible to flows that can be characterized by the following effects: downwash, wake, and venturi effects, among others. As cities continue to grow, urban planners look upward to meet the demand for more capacity. With that in mind, it is critical to consider the effects of skyscrapers in an urban environment on pedestrians.

Since the experiment is utilizing a scaled-down city model, it is important to achieve dynamic similarity. Dynamic similarity allows for the prototype city to experience corresponding forces at similar points. In order to achieve dynamic similarity, the Reynolds number needs to be the same as what the buildings would experience as a full-scale building. The Reynolds number can be calculated with equation 1 below:

$$\mathrm{Re} = \frac{\rho U_\infty L}{\mu} = \frac{\text{inertial}}{\text{viscous}} \tag{1}$$

The characteristic velocity is U, the characteristic length is L, and the dynamic viscosity is ν. The equivalent equation can be defined as, U_∞ is the free stream velocity of the fluid that is moving around the object, L is the characteristic length of the object, μ is the density of the fluid moving around the object trying to achieve dynamic similarity, and μ is the dynamic viscosity. Density and dynamic viscosity were found using the following equations:

$$\rho_\infty = \frac{1}{T}[\frac{B}{R_0} - \phi P_w(\frac{1}{R_0} - \frac{1}{R_w})] \tag{2}$$

$$\mu = \mu_{ref}(\frac{T}{T_{ref}})^{\frac{3}{2}}(\frac{T_{ref} + S}{T + S}) \tag{3}$$

Where T_{ref}, ϕ, R_0, R_w are given constants. T and P_w are the absolute temperature and value dependent on absolute pressure.

Achieving dynamic similarity allows the experiment to be comparative and analyzed as if it was carried out with a full-scale building. The way that μ is calculated can be referenced in the Laboratory Handbook for Spring 2022: ASE 120K Low-Speed Aerodynamics Laboratory pg 19, equation 8 [12].

Derived from the Bernoulli equation (4), we can calculate the wake velocity profile (5):

$$\rho_1 + \frac{1}{2}\rho v_1^2 + \rho g h_1 = \rho_2 + \frac{1}{2}\rho v_2^2 + \rho g h_2 \tag{4}$$

$$U_\infty = \sqrt{\frac{2(P_0 - P_{static})}{\rho}} \tag{5}$$

In this equation, U_∞ represents the free stream velocity, P_0 is pressure measured at a certain point on the airfoil, P_{static} is the pressure measured around the airfoil, and ρ is the density of the fluid moving around the city-scape. In this experiment, ρ is equal to the density of air.

To aid in the explanation of fluid moving through the city model, the venturi effect can characterize the behavior displayed. The Venturi effect (1a) states that when mechanical energy is constant, the velocity of a fluid passing through a constricted area increases while its static pressure decreases, for incompressible flows. The effect makes use of both the principle of continuity and the notion of mechanical energy conservation. The continuity equation for incompressible flow can be defined as:

$$A_1 v_1 = A_2 v_2 \tag{6}$$

Here, A represents the cross-sectional area that the fluid passes through and v is the velocity of the fluid.

(a) Venturi Effect **(b)** Downwash Effect

Figure 1: Flow Effects Observed in Cities

Figure 1b identifies the downwash effect on a building. Buildings create a cavity of recirculating winds in the vicinity of the structures, which causes increased vertical dispersion of wind released from structures nearby [5]. Buildings that experience downwash frequently result in higher levels of wind pollutant at the ground-level.

Regarding uncertainty, all values were calculated as per the general uncertainty equation expressed in the ASE 120K Lab Guide on page 43, equation 32 [12]. Since no system is flawless, the measurements that were obtained are the best estimate for the variable being measured and uncertainties represent the best estimate of error. Thus, the uncertainty values needed to be combined with the computed quantities to propagate the uncertainties.

3 Apparatus and Procedure

The purpose of this project was to quantitatively and qualitatively analyze flow around a configuration of wooden blocks simulating buildings in a mockup city, and to determine the implications of the resulting flow characteristics on pedestrian level wind comfort. These blocks were separated by streets such that they created a 2x2 grid formation. A smoke wand was used for flow visualization at different positions relative to the buildings. This method was used to collect qualitative data on how the flow reacted to the simulated building layout. A photo of the experimental setup is shown below.

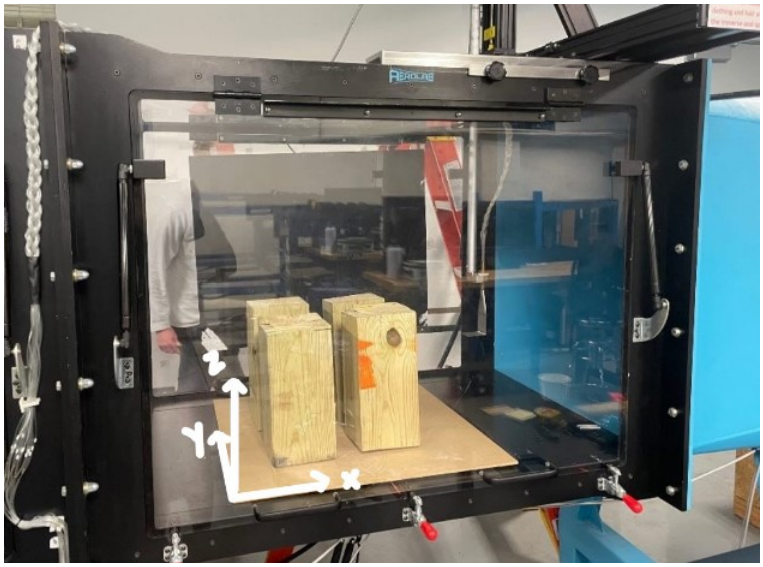

Figure 2: Photo of experimental setup showing the mockup city, wind tunnel, and pitot rake

The mockup city was constructed using four square wooden blocks with a square cross section of 5.5x5.5 inches screwed onto a 2x2 foot wooden board. These blocks were arranged in a square grid formation with a distance of 2.75 inches separating each non-diagonal block. These dimensions were determined from the ratio of the characteristic length of an average house or small building to the average width of a two lane street, which was calculated to be roughly 2:1 [8]. The physical scale of the mockup city was limited by the dimensions of the test section in the wind tunnel used. The mockup city arrangement's dimensions are visualized in the diagram below.

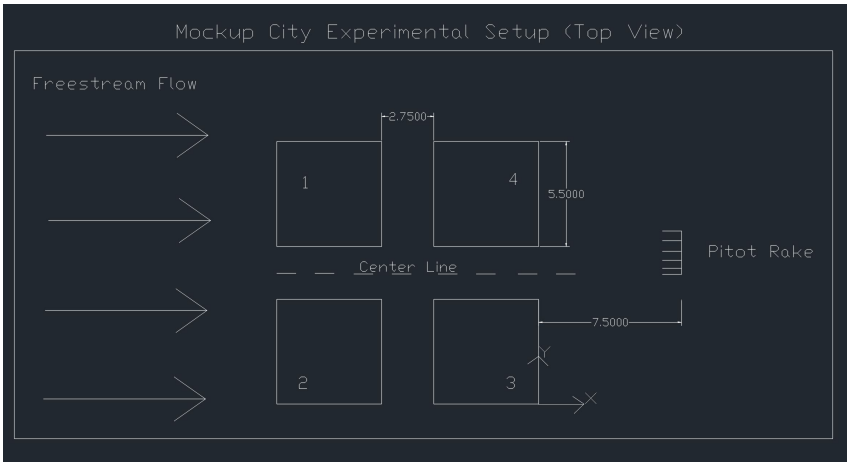

Figure 3: Top view of experimental setup with center line, dimensions in inches. Note block number labels and location of axes

For quantitative measurements a pitot rake with 18 tubes was placed downstream of the mockup city. Each pitot rake measured stagnation pressure at a frequency of 100 Hz for 5 seconds, for a total of 500 measurements per pitot tube per position. The 500 measurements were then averaged to calculate a mean value for each data point. A sweep of measurements was taken 7.5 inches behind the furthest downstream edge of the buildings across half of the mockup city to construct one half of a wake profile. Using the assumption of symmetry of flow properties over a symmetrical structure, the calculated average data points could be mirrored across the centerline to construct the entire wake profile, making measurement of the other half of the wake redundant.

After the wake data was collected, the stagnation pressure was used in Bernoulli's equation to calculate the wake velocity profile. Finally, the wake velocity profile was normalized to a nondimensional parameter, overspeed ratio, to better visualize the Venturi effect's impact on the flow through the mockup city.

This experiment was conducted in a low speed wind tunnel of contraction ratio 6:1 and turbulence intensity $\leq$0.5% RMS; the test section was 46.5 in. W, 30 in. H, and 30 in. L; finally, the wind tunnel had a two axis traverse range of motion of 22 in. W, 16 in. H, 20

in. L. This experimental setup is shown in figure 3.

4 Results

4.1 Reynolds Number Calculation

The Reynolds number was calculated from the empirical values for the density of the fluid (ρ), freestream speed in the direction of interest (u), characteristic length (L), and the dynamic viscosity (μ). For scaling, the desired Reynolds number is that of full-scale parameters, mainly a characteristic length of approximately 14 m, which was taken as the average characteristic length of a home, or small building, in America [8] the parameters rho and μ used in the full-scale Reynolds number were assumed to be equal to those in the wind tunnel, a reasonable assumption for a building in the same geographical area. Thus, the full-scale (or desired) Reynolds number is 1779300 ± 6970, while the achievable Reynolds number for the experimental model is 95625 ± 375. While these values are far off, the model's Re is close to the critical Reynolds number (Re = 100, 000); as a result, aerodynamic behavior is expected to remain fairly constant with increasing Re past $\mathrm{Re}_{\mathrm{critical}}$, as shown in the figure below, where the coefficient of drag does not change drastically after its critical value. Thus, to some degree, the results provided in this document can be extrapolated to further understand the behavior around full-scale building configurations.

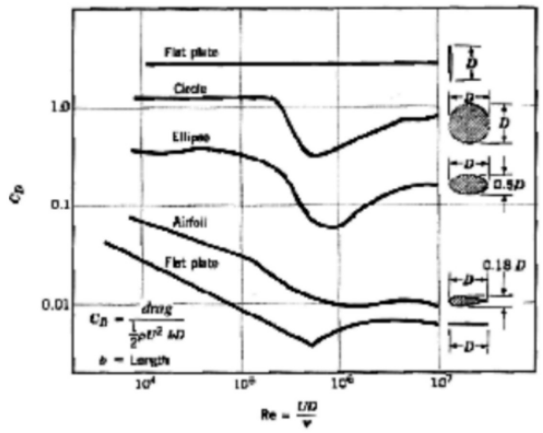

Figure 4: Coefficient of Drag Variation with Changing Reynolds Number for Different Generic Shapes, (Princeton)

4.2 Qualitative Analysis

A side-view flow visualization image using smoke-wand-generated streaklines illustrates the up-wash behavior of the flow around a formation of block structures - that is, the flow seems to turn slightly upwards as it travels downstream from the wand. Similar to flow around a blunt body or an airfoil at sufficiently high angle of attack, the flow remains attached, following the contour of the blocks for a section of its path, before separating and becoming hard to visualize. It is difficult to visualize the intensity of the down-wash effect, if there exists any at all, from the flow around a single block. This effect is quantified in the following section.

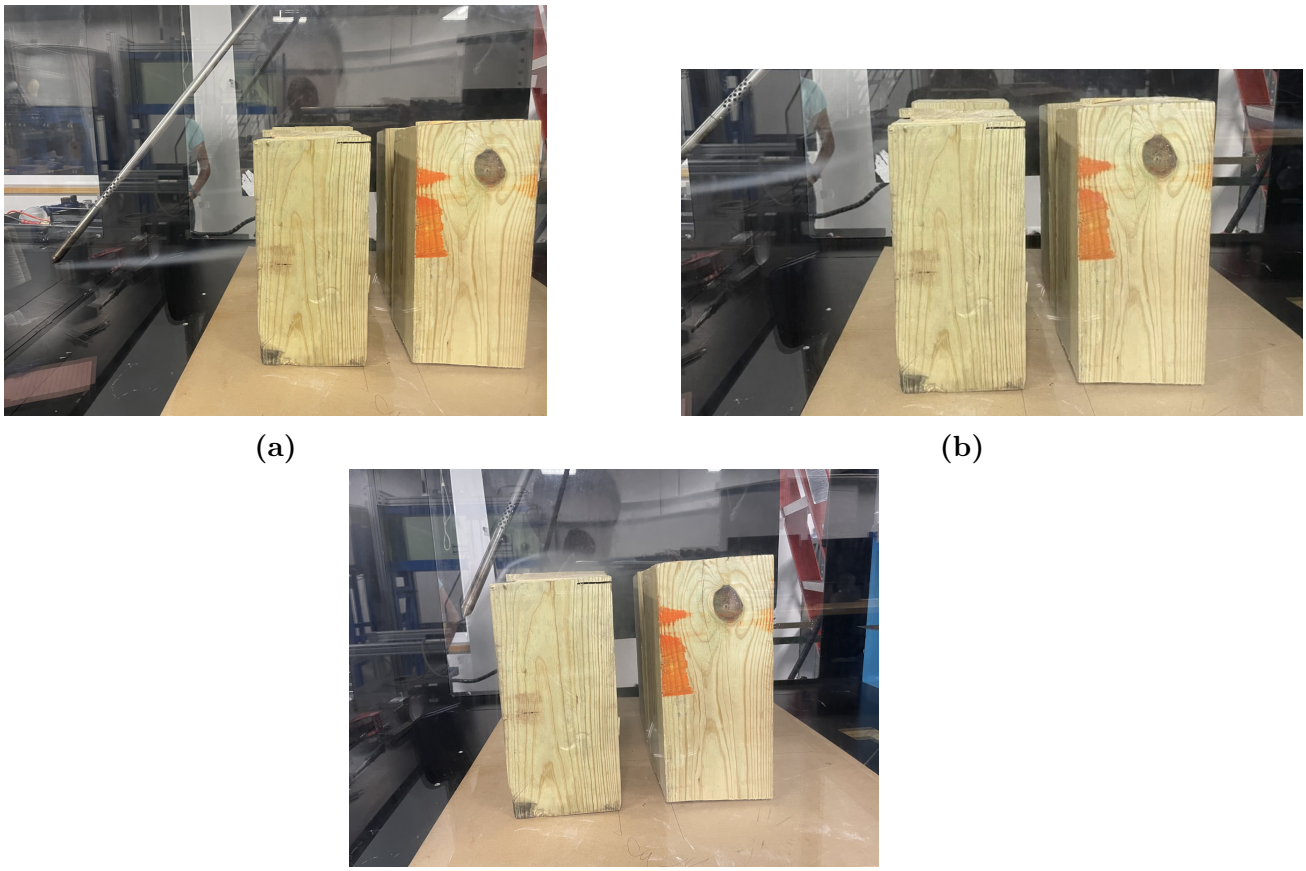

(a) **(b)**

(c)

Figure 5: Smoke Visualization at Varying Smoke Wand Heights - Streaklines

4.3 Quantitative Analysis

Wake stagnation pressure measurements were made from the center-line of the model building configuration to its right edge, assuming symmetry for measurements on the left half. The wake velocity at these points was calculated using Bernoulli's equation. By the conservation of mass equation, or continuity, it was predicted that the flow would accelerate near the center of the model (in between the blocks) due to the layout of the model effectively representing a decrease in cross-sectional area for the incoming flow. Since density is taken as a constant in the continuity equation, there is a direct inverse relation between cross section area and flow velocity. The acceleration of flow along the 'corridor region' in between

impending structures such as buildings is referred to as a funneling effect in the literature. The existence of this effect is supported by the results below.

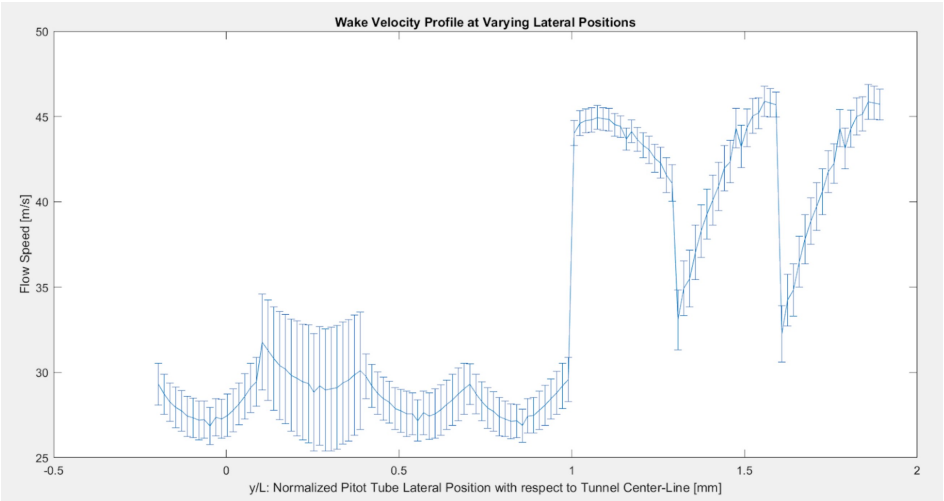

Figure 6: Flow speed vs Pitot tube lateral position from experimental data

As pitot tube position varies along 'y' from directly downstream of the outermost corner of pillar 3 (as defined in figure 2) to directly on the centerline of the model, the velocity increases drastically and suddenly at y/L = 1. Given that L is the characteristic length of the model building (also its width), this indicates a sharp increase in flow velocity at the edge of the building, as predicted by this experiment's hypothesis.

For physical interpretation, the data can be normalized by the following formula, which describes the overspeed ratio, or the degree to which the local flow exceeds a reference velocity, Va. Here, Va is taken as the velocity that would exist at a given height on an open field at the given free stream velocity - i.e. the hypothetical completely unobstructed free stream velocity.

$$\text{Overspeed ratio: } K = \frac{V}{V_a} \tag{7}$$

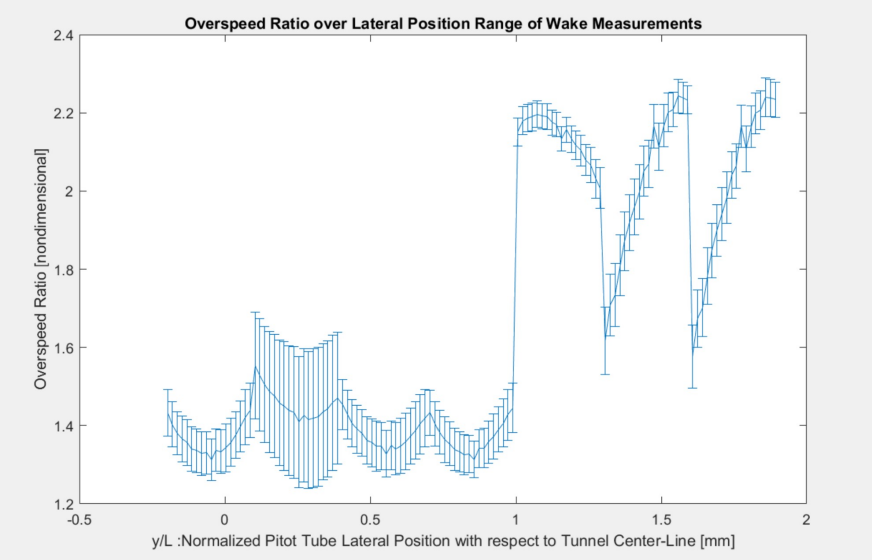

Figure 7: Overspeed ratio vs Pitot tube lateral position from experimental data

Analysis of the oscillatory behavior of the wake velocity profile is beyond the scope of the analytical methods presented in this document. While the main pattern in the flow is described by the Venturi effect, which can be described entirely by the continuity equation, the data also shows secondary behavior that should be studied with computational methods: sidewash and downwash are some of the simpler ones, and they both may cause intermittent fluctuations in the local velocity, which could explain the oscillating behavior seen in the graph above. Moreover, the larger the configurations of buildings, the more complex flow interactions become, combining all of these effects and others to produce non-uniform behavior.

4.4 Implications to Pedestrian Level Wind Comfort

Under the assumption that aerodynamic behavior would not change much between Re = 95625 $\pm$ 375 and Re = 1779300 $\pm$ 6970, the results can be used to predict full-scale flow behavior around a similar configuration of buildings: equally spaced buildings of equal height, proportionally scaled up. From figure 7, the flow near the centerline of the model,

at $\frac{y}{L} > 1$, is more than doubled in speed with respect to the reference velocity, featuring a maximum over-speed ratio of K = 2.2428 ± 0.0568. Thus, for an unobstructed free stream velocity of 5 m/s, a frequent occurrence in reality, local speeds could reach velocities above 10 m/s, which is much above the established pedestrian level comfort limits of 3.8 m/s for standing and 5.5 m/s for standing. For this reason, it seems that the experimental model, in all its simplicity, is not aerodynamically favorable for real-world applications. This highlights the importance of wind engineering in designing city layouts that minimize the undesirable effects outlined in this document.

5 Summary and Conclusions

The results of this experiment align with the flow behaviors discussed in literature. The observations show the upwash effect through the upward slope of the flow going downstream visualized with the smoke wand, which, along with the analogous effect of downwash, is prevalent in urban flows. Furthermore, looking at the wake velocity profile, the Venturi effect can be observed by the increased velocity of the flow in the region between two buildings as the flow is forced into a smaller cross-sectional area. The Venturi effect is known to play a significant impact on pedestrians as the wind velocity is forced to increase on city streets flanked by tall buildings on all sides, making it difficult to walk or stand on the pavement, so the data from this experiment is as expected in comparison to effects observed in reality.

However, these results have a number of limitations. Firstly, since the experimental Reynolds number is significantly lower than the desired value, any conclusions drawn from the presented data rely on the assumption that, since the experimental Reynolds number is so close to the critical Reynolds number, the empirical flow patterns will conserve similarity at higher Reynolds number. Further experimentation can determine whether this assumption holds as the freestream velocity is increased past the tested regime. Additionally, the velocity

profile was taken at a relative altitude much higher than reasonable for pedestrian-level flow due to equipment limitations; as a result, the velocity profile taken at this altitude may not be representative of the behavior at pedestrian level. While the observations at the different altitudes indicate minimal differences in flow behavior, it may impact the velocity distribution in an unpredictable manner. Hence, the findings of this experiment are better applied to future applications of low-altitude flight, such as shipping drones, rather than at pedestrian levels.

Another factor that must be considered is thickness of the boundary layer. The lowest height for the boundary layer of the Earth's atmosphere is considered to be 3,300 ft [7], which is far above the height of even the tallest skyscrapers. However, since a boundary layer analysis was not performed for the wind tunnel, it is likely that this experimental study did not account for the effects of the boundary layer, so this is another limitation of this experiment. Lastly, the angle the wind hit the front face of the skyscrapers was at a 90 degree angle; in real-life, with all the variance in weather and atmospheric conditions, it is unlikely that wind will approach cities at the angle analyzed in this experiment.

Future studies to further investigate urban flow behavior could account for some of the aforementioned limitations. One study could design a model or experiment such that the Reynolds number is closer to or matches that seen in real-life. Another option would be to design an experiment that more deeply analyzes the velocity profile and flow behavior at varying altitudes to determine whether there are significant differences between pedestrian-level and low-altitude-flight-level flow behavior. A third study could analyze flow behavior of freestream velocity at different angles relative to the buildings. Because of the complicated relationships between the various flow effects, a model using computational fluid dynamics methods would significantly improve the understanding of flow behavior around various city configurations and aid in discovering approaches to help increase pedestrian-level comfort in cities as the numbers and sizes of skyscrapers increase exponentially around the world.

6 References

[1] ANDERSON. *Fundamentals of Aerodynamics*. 6th ed., McGraw-Hill Education, 2016.

[2] Barr, J. (2018, January 2). Why was 2017 another record-breaking year for skyscrapers? Building the Skyline. Retrieved May 6, 2022, from https://buildingtheskyline.org/global-skyscraper-growth/

[3] Chen, J., Gianfelice, M., Izukawa, N., Elshaer, A., Aboshosha, H. (2021, February 4). Run-time and statistical pedestrian level wind map for Downtown Toronto. Frontiers. Retrieved May 6, 2022, from https://www.frontiersin.org/articles/10.3389/fbuil.2021.603836/full

[4] Drag of blunt bodies and streamlined bodies. (n.d.). Retrieved May 6, 2022, from https://www.princeton.edu/~asmits/Bicycle_web/blunt.html

[5] EPA. (n.d.). Issues Related to Building Downwash in AERMOD. EPA.gov. Retrieved May 6, 2022, from https://www.epa.gov/sites/default/files/2021-01/documents/downwash_overview_white_paper.pdf

[6] Fairclough, C. (n.d.). Exploring the Venturi effect. COMSOL. Retrieved May 4, 2022, from https://www.comsol.com/blogs/exploring-the-venturi-effect/#:~:text=The%20Venturi%20effect%20states%20that,of%20conservation%20of%20mechanical%20energy.

[7] Harvey, C. (2019, 19 November). The World's Winds are Speeding Up. Retrieved May 6, 2022 from: https://www.scientificamerican.com/article/the-worlds-winds-are-speeding-up/

[8] Joint Center for Housing Studies. (June, 2021). *Median size of single family housing unit in the United States from 2000 to 2020*. Satista. from https://www.

statista.com/statistics/456925/median-size-of-single-family-home-usa/#:~:text=Median%20size%20of%20single%20family%20house%20in%20the%20U.S.%202000%2D2020&text=The%20average%20single%20fam

[9] Nanowski , N. (2019, April 3). It's not in your head, Toronto's tall towers are making the wind worse — CBC News. CBCnews. Retrieved May 3, 2022, from https://www.cbc.ca/news/canada/toronto/wind-toronto-buildings-skyscrapers-construction-1.5079986

[10] Pielke, R. A. and Hayden, . Bruce P. (2016, November 16). planetary boundary layer. Encyclopedia Britannica. https://www.britannica.com/science/planetary-boundary-layer

[11] Stevens, G. (2020, April 16). Wind effects in urban areas. LinkedIn. Retrieved May 3, 2022, from https://www.linkedin.com/pulse/wind-effects-urban-areas-george-stevens/

[12] Tinney, C. E., et al. Austin, Texas: University of Texas at Austin, 2022. Print.

[13] Wu, H. (1994). Pedestrian-Level Wind Environment around Buildings. Concordia University. Retrieved from NN90909.pdf (concordia.ca)

A Uncertainty Calculations

All uncertainty values were propagated from baseline values for quantities that were directly measured during the experiment, such as the stagnation pressure measured by the pitot rake in the wake region of the model. Such baseline uncertainties were taken as the standard deviation of all trials of a certain measurement (such as the standard deviation of all 500 PTA measurements at a specific point) or the systematic uncertainty inherent to the measurement device used, whichever was greater. For reference, the uncertainty associated with a measurement device is given by the smallest numerical increment for a digital device and half of the smallest increment for an analog device. From these baseline values, uncertainty was propagated to all other variables by the Kline and McClintock simplification of the general uncertainty propagation formula presented in the ASE120K lab guide [12].